UNIVERSITY OF PITTSBURGH

ORTHOPAEDIC ROBOTICS LABORATORY

2017 SUMMER UNDERGRADUATE ABSTRACT BOOKLET

PITT | SWANSON ENGINEERING
BIOENGINEERING

FOREWARD

The Orthopaedic Robotics Laboratory is the University of Pittsburgh's collaborative effort between the Department of Bioengineering and Department of Orthopaedic Surgery. The mission of the ORL is the prevention of degenerative joint diseases by improving diagnostic, repair, and rehabilitation procedures for musculoskeletal injuries using state-of-the-art robotic technology. The ORL would like to commend the work of the undergraduate students during the summer of 2017. Students made significant impacts in the study of hand, shoulder, elbow, and knee joint diseases. The work of our students, with the help of our mentors, contributes greatly to world of Orthopaedic Research and to all patients who benefit.

OUR TEAM

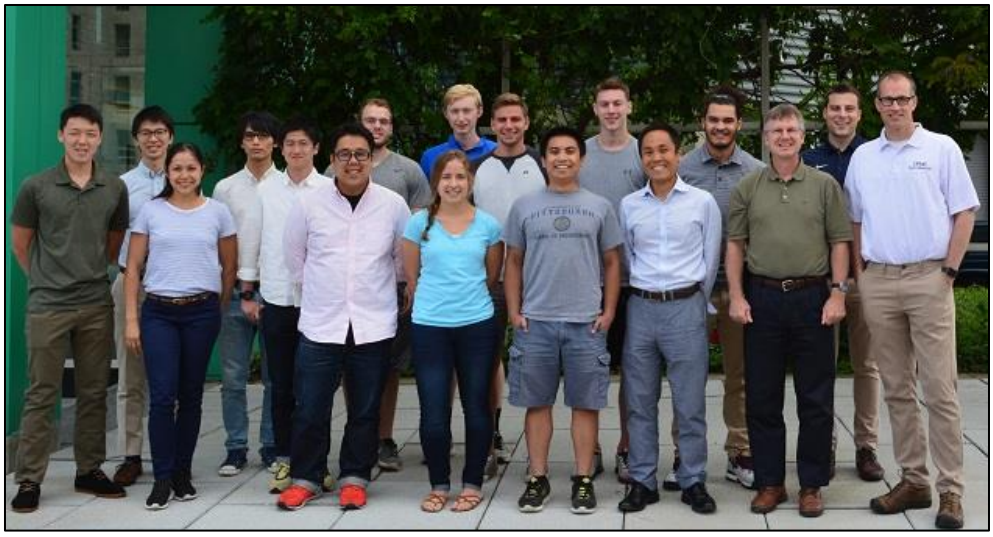

Ryan Black
Class of 2018
Bioengineering
University of Pittsburgh

Catherine Smith
Class of 2019
Bioengineering
University of Pittsburgh

Benjamin Roadarmel
Class of 2019
Bioengineering
University of Pittsburgh

James Gorenflo
Class of 2018
Mechanical Engineering
University of Pittsburgh

Joseph Greaves
Class of 2019
Bioengineering
Penn State University

TABLE OF CONTENTS

Comparison of Screw Quantity and Placement of Metacarpal Fracture Fixation: A Biomechanical Study

Ryan Black [1]; Stephen Canton [2]; Richard E. Debski [1,2]; John Fowler [2]
1. Department of Bioengineering, University of Pittsburgh, Pittsburgh, PA, United States
2. Department of Orthopaedic Surgery, University of Pittsburgh, Pittsburgh, PA, United States

INTRODUCTION: In the US, there is an estimated total of 3,468,996 upper extremity injuries per year [1]. The second most common type of upper extremity fractures are phalangeal and metacarpal fractures [2]. The most popular choice of metacarpal fracture fixation is dorsal plating [3]. The AO foundation (Association for the Study of Internal Fixation) recommends a total of 6 bicortical screws proximal and distal to the fracture for long bone fractures [4,5]. However, many metacarpal fractures do not allow for 6 screws of plate fixation due to size limitations and surrounding soft tissues [6]. Recent studies have shown that strategic placement of fewer screws can provide comparable fixation strength to 6 screw constructs and preserve desired clinical outcomes [6,7,8,9,10]. It has been shown that when varying the number of screws, 4 locked and 6 non-locked bicortical screws demonstrated comparable fixation strength [6]. However, it is not known how the fixation strength will compare between fracture fixations with different screw quantities when using the same plate and screw type. Therefore, the objective of this study is to determine the structural properties of non-locking dorsal plate fixation with 4 vs. 6 bicortical screws.

DEVELOPMENT OF PROTOCOL: Fourth-generation composite biomechanical testing grade third metacarpal sawbones (Sawbones Model 3416; Pacific Research Laboratories, Vashon, WA, USA) were selected for this study instead of cadaveric metacarpals to minimize inter-specimen variability in mechanical properties and geometry [11]. To assess differences in fixation strength between the 4 and 6 screw constructs, a cantilever bending test in the apex dorsal direction was selected to simulate the moment generated by the hand flexor tendons on the distal head of the metacarpal [11,12]. A cyclic loading protocol was chosen to simulate increasing use of the wrist during the fracture healing period and rehabilitation. The cyclic loading consists of three sets of 100 cycles: 5-40N to simulate active flexion of the hand with minor resistance, 5-70N to simulate a strong composite grasp, and 5-100N to simulate a firm fingertip pinch [12,13,14]. Following cyclic loading, the metacarpals will be loaded to failure to determine the structural properties of the fixation constructs. In addition, an optical tracking system (Spicatek, Haiku, HI, USA) will be utilized to determine deflection along the fixation construct during load-to-failure.

TESTING APPARATUS: The cantilever bending tests will be performed using custom clamps for a uniaxial materials testing machine (Instron Model 5960, Norwood, MA, USA) (Figure 1) [11,12]. Prior to testing, the stiffness of the custom clamps was assessed to ensure the deflection of the clamps during the loading protocol will be negligible compared to the deflection of the fixation constructs. To ensure minimal deflection of the clamps, the stiffness of the clamps must be approximately two orders of magnitude greater than the stiffness of the metacarpal. The expected stiffness of the metacarpal fixation construct is 30-40 N/mm [12]. Figure 1A depicts the original custom clamps (Stiffness = 293.8N/mm). Figure 1B depicts the modified custom clamps with the larger base below the clamp. The modified clamps' stiffness was 1159.5 N/mm, approximately two orders of magnitude greater than the fixation constructs, meeting the initial criteria.

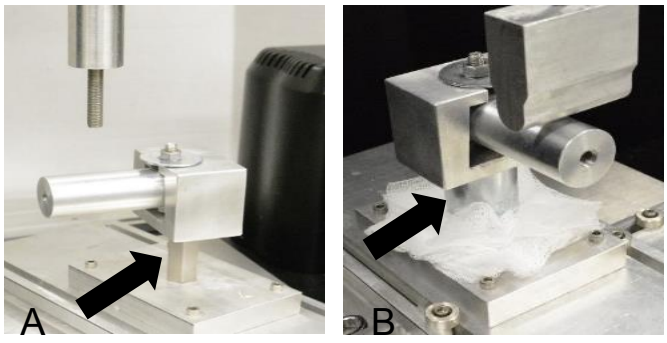

Figure 1: A) Original clamps used for cantilever bending. B) Modified clamps used for cantilever bending. The modified cylindrical base is shown with the black arrows.

STRUCTURAL PROPERTIES OF INTACT METACARPAL: Prior to testing any fixation constructs, an intact metacarpal was tested to determine the structural properties of the sawbone

metacarpal, as well as practice the overall protocol. Using Bondo (3M, Minneapolis, MN, USA), 1.7cm of the proximal end of the metacarpal was potted into our custom clamps for cantilever-bending (Figure 2) [12]. Five white optical tracking beads were attached along the metacarpal to track deflection. The metacarpal was then mounted in custom clamps and cantilever bending tests were performed. A 5N preload was applied to the metacarpal 6.2cm away from the proximal end [12,15]. The metacarpal was then preconditioned from 5-15N for 10 cycles at 20 mm/min. After preconditioning, the metacarpal was cyclically loaded using the protocol described earlier.

The stiffness of the intact metacarpal was determined to be 144.0 N/mm, while the maximum deflection was 1.8mm. The stiffness of the intact metacarpal is an order of magnitude higher than the expected stiffness of the metacarpal fixation construct (30-40N/mm) [12]. However, the deflection of the metacarpal was similar to values reported in previous studies [11,12]. Overall, the practice test was successful and the structural properties of the intact sawbone metacarpal were determined.

PRELIMINARY TESTS WITH FIXATION CONSTRUCTS: After testing an intact metacarpal, two preliminary tests were performed using a 6 screw and 4 screw construct. A midshaft transverse fracture was created using an oscillating saw. Each sawbone was plated with a 6-hole nonlocking plate (2.3mm Stryker Profyle Plate, Kalamazoo, MI, USA). After fracture fixation, 1.7cm of the proximal end was then potted using Bondo (3M, Minneapolis, MN, USA) into our custom block for cantilever-bending [12]. A total of 10 white optical tracking beads were attached to the sawbone-plate construct for optical tracking of the construct deflection, with 5 beads attached to both the sawbone and plate.

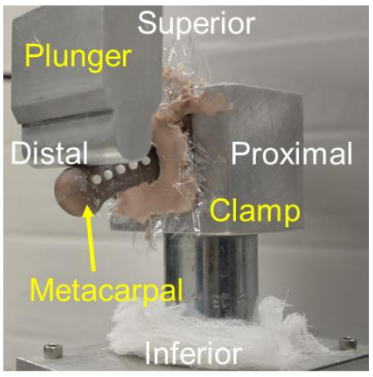

Figure 2: Custom clamps used to perform cantilever bending tests using a materials testing machine.

The metacarpals were then mounted in custom clamps and cantilever bending tests were conducted using a materials testing machine (Instron Model 5960, Norwood, MA, USA) (Figure 1) [11,12]. The metacarpals were tested both in cyclic loading and load to failure [12, 15].

From the two preliminary tests performed, the 6 screw construct demonstrated a higher stiffness and ultimate bending load than the 4 screw construct. In addition, the 4 screw construct demonstrated a larger maximum deflection compared to the 6 screw construct. However, the deflections observed were higher than those reported in the literature [11,12].

# of Screws	Stiffness (N/mm)	Maximum Deflection (mm)	Ultimate Bending Load (N)
4	40.7	9.5	147.9
6	67.7	4.0	256.4

Table 1: Results of two preliminary tests performed with 4 and 6 non-locking bicortical

DISCUSSION: From the two preliminary tests, the stiffness of the clamps are two orders of magnitude greater than the stiffness determined for the 4 and 6 screw metacarpal fixation constructs, meeting the previously set criteria. However, it was also determined from preliminary tests that the potting material may not be stiff enough for the loading protocol, therefore contributing to the overall construct deflection. As a result, the maximum deflections of the 4 and 6 screw constructs were much larger than those reported previously [11,12]. Overall, the practice and preliminary testing provided valuable information about problems with the initial experimental design and protocol. In the future, more preliminary testing will be conducted with an updated experimental design and protocol, specifically stiffer potting material will be utilized to minimize its impact on the measurement of metacarpal deflection.

ACKNOWLEDGEMENTS: Support from the University of Pittsburgh Department of Bioengineering, Swanson School of Engineering, and the Department of Orthopaedic Surgery is gratefully acknowledged.

REFERENCES: [1] Ootes et al. Hand (N Y) 2012. [2] Karl et al. JOT. 2015. [3] Firoozbakhsh et al. JHS. 1996. [4] Helfet et al. JBJS. 2003. [5] Berkes et al. CRMM. 2013. [6] Barr et al. Hand (N Y). 2013. [7] Hak et al. JOT. 2010. [8] Tornkvist et al. JOT. 1996. [9] Afshar et al. JHS(E). 2011. [10] Ochman et al. JHS. 2010. [11] Sohn et al. JHS. 2008. [12] Tannenbaum et al. JHS. 2017. [13] Powell et al. JHS(E). 2004. [14] Strickland. JHT. 2005. [15] Dahl et al. JHS. 2012.

Biomaterial Repair of the Rat Supraspinatus Tendon Enthesis

Catherine A. Smith[1]; Gerald A. Ferrer[1]; João Novaretti[2]; Benjamin B. Rothrauff[2]; Rocky Tuan[2]; Volker Musahl[2,1]; Richard E. Debski[1,2]

[1]Department of Bioengineering & [2]Department of Orthopaedic Surgery, University of Pittsburgh, Pittsburgh, PA, United States

INTRODUCTION: Rotator cuff injuries are a highly prevalent and significant clinical problem in the general population. Though surgical repair of small tears has been shown to be clinically successful, there is up to a 94% re-tear rate with larger tears [1]. High re-tear rates may be a result of the poor innate healing capacity of the rotator cuff enthesis [2], Current methods of augmenting healing at the enthesis include allografts, extra-cellular matrix (ECM), platelet rich plasma (PRP), growth factors and stem cells [3]. Several biomaterials have been investigated to assess the structural properties in healing rat rotator cuffs with promising results, including bone marrow derived stem cells (MSCs) transduced with scleraxis, and fibroblast growth factor (FGF-2) [4,5]. However, the ideal biomaterial or combination of biomaterials to augment healing of rotator cuff repair surgery is unknown. The objective of this study was to assess the effects of different biomaterials (fibrin, GelMA, ADSCs and TGFβ) alone and in combination on the tensile properties of healing rat rotator cuff tendons.

METHODS: One hundred and twenty-nine fresh-frozen rat humeri were evaluated following a full-thickness transection of the supraspinatus and infraspinatus tendons after 4 weeks of healing. The 8 treatment groups for the rotator cuff injuries included: no repair, repair only, fibrin, GelMA, fibrin + adipose derived stem cells (ADSCs), GelMA + ADSCs, fibrin + ADSCs + TGFβ, and GelMA + ADSCs + TGFβ. The eight groups were further divided into two sub-groups of 1) Acute: tears created and immediately repaired with 4 weeks of healing and 2) Chronic: tendons were injected with botulinum toxin to induce fatty degeneration, tear created, 8 weeks of caged activity, repair, and 4 weeks of healing [6].

Each specimen was thawed at room temperature and the humeral head was cerclaged to prevent humeral head avulsion. Supraspinatus tendons were kept hydrated with physiologic saline solution, gripped using custom clamps and mounted in a materials testing machine (Instron, Model 5965, Norwood, MA, USA) equipped with a 50N load cell. The experimental protocol consisted of a 0.2N preload, preconditioning between 0.2-1N for 10 cycles, and a load-to-failure test. All tests were performed at an elongation rate of 5mm/min. The structural properties (ultimate load, ultimate elongation, stiffness and energy absorption to failure) were determined from the load-elongation curve. A chi-square test was performed to evaluate the effect of the biomaterials on the failure mode. A two-tailed independent t-test was performed to compare chronic and acute tear groups (combining all treatment groups together) on each structural property. A one-way ANOVA with a post-hoc Bonferroni test was performed to assess the effect of the different treatment groups on each structural property. Significance was set at $p < 0.05$.

RESULTS: The most common failure modes among all groups were either at the enthesis or midsubstance. Treatments involving GelMA failed at the enthesis at a higher frequency than treatments involving fibrin ($p < 0.05$). Treatment groups that utilized GelMA had a failure rate at the enthesis of 43.2% while groups using fibrin failed at the enthesis only 23.4% of the time. No intact controls failed at the enthesis. When combining all treatment groups together, chronic tears had significantly lower ultimate load (26%) and energy absorption to failure (36%) compared to acute tears ($p < 0.05$). No difference between treatment groups was found for ultimate load, ultimate elongation, stiffness or energy absorption to failure ($p > 0.05$). However, intact controls were found to have a significantly greater ultimate load and stiffness than all treatment groups. Ultimate load for intact controls were 248% greater than the treatment groups for chronic tears (Figure 1). Similarly, stiffness for intact controls were 597% greater than the treatment groups for chronic tears (Figure 2). No difference was found between the treatment groups and intact controls for

ultimate elongation and energy absorption to failure.

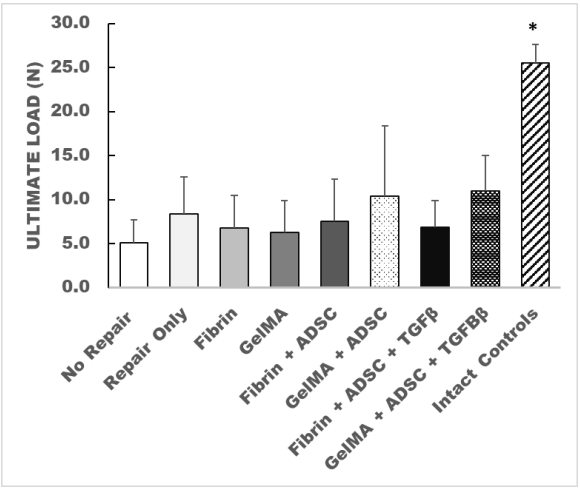

Figure 1: Ultimate Load for all treatment groups with chronic tears. * Control group significantly greater than all treatment groups ($p < 0.05$).

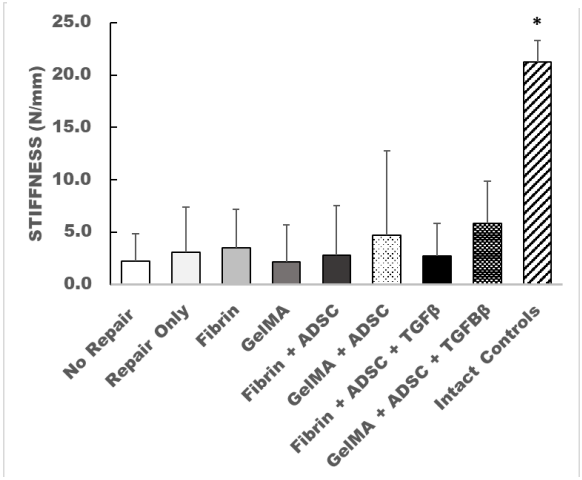

Figure 2: Stiffness for all treatment groups with chronic tears. * Control group significantly greater than all treatment groups ($p < 0.05$).

DISCUSSION: The finding that GelMA causes the tendons to fail at the enthesis most often indicates that some biomaterials might better strengthen the enthesis than others, ie, fibrin may strengthen the enthesis better than GelMA. Consistent with previous studies, the chronic tears were weaker than acute tears in terms of having a lower ultimate load, supporting the validity of the rat model used [6,7]. The results show no statistical difference between the treatment groups for all structural properties, indicative that the biomaterials used are able to restore the site of injury to a similar degree. Differences between this study and others may be attributed to the specimen preparation, test setup, healing time and injury model used. For example, surgical repair of a two-tendon cuff tear in a rat and subjective delineation of the healing supraspinatus and infraspinatus tendon may introduce variability in the results of structural properties of the healing complex. Despite variability in the results, previous studies that used a chronic massive cuff tear rat model and investigated the structural properties of the healing rotator cuff also found large variability and had similar findings [6,7]. Therefore, to improve upon the current study, future studies will investigate the mechanical properties of the tendons to better assess the quality of the healing tissue. Since the current animal model may be too small to detect differences for a chronic massive cuff tear, future work will also use a larger animal model (e.g. sheep) to increase the likelihood of detecting differences between treatments.

SIGNIFICANCE: The biomaterials considered in this study are equally viable options to augment tendon healing, though fibrin strengthened the enthesis more than GelMA.

REFERENCES: [1] Galatz et al. JBJS. 2004 [2] Angeline & Rodeo. Clin Sports Med. 2012 2014 [3] Montgomery et al. Curr Rev Musc Med. 2011 [4] Gulotta et al. AJSM. 2011 [5] Ide et al. JSES. 2009 [6] Killian et al. AJSM. 2015 [7] Killian et al. JOR.

ACKNOWLEDGEMENTS: Support from the University of Pittsburgh Swanson School of Engineering, Department of Bioengineering, Department of Orthopaedic Surgery, and NSF Fellowship Grant No. 1247842 is gratefully acknowledged.

Orientation of Non-Recoverable Strain in the Glenohumeral Capsule Does Not Change Following Multiple Dislocation

Benjamin Roadarmel[1, 3], Tetsuya Takenaga[1, 2], Masahito Yoshida[1, 2], Calvin A. Chan[1, 2]
Volker Musahl1[2, 3], Richard E. Debski[1, 2, 3], Albert Lin[1, 2]
1 Orthopaedic Robotics Laboratory, University of Pittsburgh, Pittsburgh, PA USA; 2 Department of Orthopaedic Surgery, University of Pittsburgh, Pittsburgh, PA USA; 3 Department of Bioengineering, University of Pittsburgh, Pittsburgh, PA USA

INTRODUCTION: Arthroscopic Bankart repair is generally the first choice for surgery to treat anterior shoulder instability [1], however, Bankart repair still fails to prevent reoccurrence in up to 22% of patients [2]. In addition to Bankart lesions, the capsule experiences non-recoverable strain after subluxation or dislocation of the glenohumeral joint [3]. Capsular plication can be performed during arthroscopic Bankart repair to reduce the volume of the glenohumeral capsule and help decrease the chance of reoccurring shoulder instability. However, plication is generally preformed based on the surgeon's experience with little information on the optimal direction for plication. The objective of this study is to determine the direction of non-recoverable strain in each region of the glenohumeral capsule after multiple dislocations.

METHODS: Eight fresh-frozen cadaveric shoulders (age range 49-59 yrs) were dissected free of all soft tissue except the glenohumeral capsule. A 7 x 11 grid of strain markers was affixed to the anterior and posterior band of the inferior glenohumeral ligament (IGHL), and the axillary pouch. The position of the markers while the capsule was inflated with minimal pressure served as the reference state. The humerus and scapula were then mounted in a 6 degree of freedom robotic testing system. At 60 degrees of abduction and 60 degrees of external rotation of the glenohumeral joint, an anterior load was applied to reach an anterior translation of one half the maximum AP width of the glenoid plus 10 mm. This definition of dislocation resulted in non-recoverable strain and a reproducible Bankart lesion. Following 1, 2, 3, 4, 5 and 10 dislocations, the positions of the strain markers were again recorded with the capsule inflated. The difference in these positions compared to the reference state defined the non-recoverable strain, represented by the maximum principal strain calculated using ABAQUS (ABAQUS/CAE Student Version 6.4; Simulia, Providence RI).

Any maximum principle strain vectors with a magnitude less than 3% were removed from further analysis as that is the repeatability of the entire process [4]. The inferior glenohumeral capsule was divided into an anterior and posterior region by using the column of markers placed at the 6 o'clock position of the glenoid. A 2-D projection of each anterior and posterior strain map was then generated by orienting the model to mimic the view of a surgeon preforming Arthroscopic Bankart repair. The angle of deviation between each of the maximum principle strain vectors and the AB-IGHL or PB-IGHL for the anterior and posterior regions of the capsule respectively, were measured using ImageJ software (National Institute of Health, Bethesda, MD, USA). The capsule was split into four sub-regions, the anterior band of IGHL (AB), anterior axillary pouch (AA), posterior axillary pouch (PA), and the posterior band of IGHL (PB). Circular statistics compared the direction of the maximum principal strain between groups and dislocations. To be included in a statistical test, the sub-region must have at least five angular values as well as be non-uniform and follow a Von Mises distribution. Rayleigh's test and Kuiper's test were used to determine non-uniformity and normality, respectively. A Watson-Williams test was then used to detect differences in the mean angle between dislocations, sub-regions, and specimens. Significance was set to $p < 0.05$. P-values from the Watson-Williams test were corrected for multiple comparisons using the false discovery rate method.

RESULTS: Direction of maximum principal strain was similar after all dislocations within each specimen (Fig 1). The mean angles of a representative specimen for the anterior axillary pouch sub-region were equal to 16, 27, 29, 20, 27, and 35 degrees for the first, second, third, fourth, fifth, and tenth dislocation, respectively. These means did not significantly differ ($p > 0.05$) and this result was typical in 75% of the comparisons examined. However, the mean angles were significantly different when comparing between sub-regions within a specimen as well as when comparing between specimens. The mean angles

from three sub-regions of a representative specimen where equal to 8, 168, and 122 degrees (Fig 2-A), while the mean angles for the anterior axillary pouch from six specimens was equal to 73, 27, 18, 168, 85, and 132 degrees (Fig 2-B). Both comparisons were significantly different ($p < 0.05$), which was typical of more than 70% of comparisons examined in both cases.

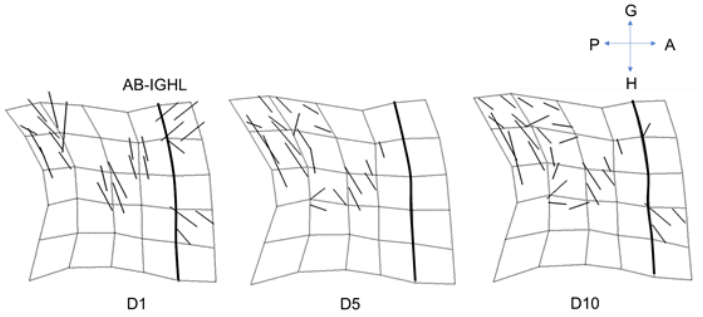

Figure 1. Fringe plots of direction of maximum principal strain generated for the anterior region of the inferior glenohumeral capsule for a typical specimen after the A) first, B) fifth, and C) tenth dislocation. AB-IGHL (Anterior Band of Inferior glenohumeral ligament) A (Anterior) P (Posterior) G (Glenoid) H (Humeral)

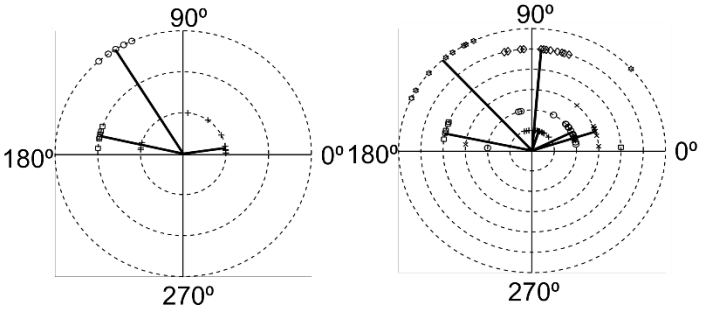

Figure 2. A) Circular plot showing angle distribution and mean angles of non-recoverable strain for Anterior Band (square), Anterior Axillary Pouch (diamond), and Posterior Band (circle) sub-regions of specimen 4 after the first dislocation. B) Circular plot showing angle distribution and mean angles for the anterior axillary pouch region for each specimen. Data points represent distribution on each circle for a specimen, specimen 6 and 8 are not included due to lack of data.

DISCUSSION: The direction of maximum principle non-recoverable strain remains the same after multiple dislocations meaning that a patient having experienced reoccurrence has not significantly altered the optimal direction for plication. However, significant differences exist between the different sub-regions suggesting that not only should the axillary pouch regions be plicated, but each region may have to be addressed separately. Many significant differences were also found between specimens meaning that determining the optimal direction for capsular plication may require individualized repair. This large variation is consistent with a previous study done to determine non-recoverable strain in the glenohumeral capsule following subluxation [3]. In the future, individual parameters that may affect the direction of non-recoverable strain should be determined and a clinical evaluation that can be performed to help clinicians determine the optimal direction for capsular plication should be developed.

SIGNIFICANCE: The optimal direction for glenohumeral capsular plication for a patient does not change due to re-dislocation. However, the optimal direction will differ greatly between patients and with the anterior and posterior regions of the capsule requiring a more individualized surgery.

REFERENCES:

[1] An JSES 2016
[2] Bessiere CORR 2014
[3] Malicky JBE 2001
[4] Moore JOR 2008

Design of an Elbow Testing Apparatus to Simulate Flexion in Varying Degrees of Shoulder Abduction

James Gorenflo, John Fowler, AJ Blackburn, Robert Kaufmann, Richard E. Debski
Orthopaedic Robotics Laboratory, Department of Bioengineering, University of Pittsburgh, PA, USA

Introduction: *In-vitro* joint simulators have been developed in order to reproduce the active kinematics and dynamic loads of the upper and lower extremities. The simulation of active joint motion is useful to evaluate surgical procedures, improve rehab protocols and to further the understanding of physiological movement. With respect to the elbow joint, several studies already reliably reproduced active flexion. Previous literature has mainly focused on the varus, valgus and vertical loading effects on the elbow joint. However, there have been no studies of the elbow joint while also abducting the shoulder. The biomechanics of the elbow are altered when rotated through shoulder abduction due to different orientations of gravitational force. Therefore, the dynamic loading required to produce elbow flexion will change as the shoulder progresses through different positions. The Shoulder Testing Apparatus Revision IV (STAR IV) was originally built to simulate joint kinematics of the shoulder but now it has the ability to test the kinematics of the knee joint. Utilizing six actuators and a pulley system, the STAR IV is capable of dynamically controlling cables that are attached to muscle tendons of the shoulder or knee joint. With some modifications, it is possible to use this device to simulate varying degrees of shoulder positions while actively flexing the elbow joint. The objective of this project is to design an apparatus to allow simulation of muscle forces about the elbow and determine required force parameters to serve as input.

Design Criteria: The current STAR IV has a mounting system that can fix and rotate the humerus to simulate shoulder abduction (Figure 1). Six actuators will be used to dynamically control the biceps, brachialis, brachioradialis, triceps, flexor pronator mass, and the extensor tendons. The muscles from the flexor pronator mass and the extensor tendons will each be treated as one group since all of the muscles originate from the medial and lateral epicondyle respectively. Customized pieces must be rigidly fixed onto the mount and be capable of maintaining alignment through varying degrees of shoulder abduction. In addition to maintaining the proper directions, the correct contributions of each muscle must be considered to accurately reproduce active flexion. The configuration of the alignment and pulley system must not constrain the motion of the elbow. In addition, the upper extremity should not have any external forces or torques acting on it to prevent any undesired stress or motion in the arm.

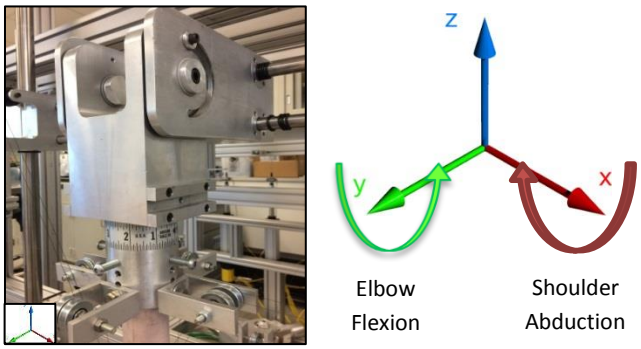

Figure 1: Elbow Flexion will occur about the y-axis and the device will rotate about the x-axis to simulate shoulder abduction.

Final Design: The alignment system consists of the upper and lower alignment pulley systems. All parts are made symmetrically which grants the ability to use a right or left arm in the testing system. In the upper alignment system, four base plates are bolted into the cylindrical mount that have holes in the side for pulley rods and holes in the top for the attachment of the lower alignment system. The concave shape of the base plates creates a rigid structure when mated with the cylindrical humerus mount. Then, the tightening of hex nuts on the pulley rods provides additional clamping force for extra rigidity. This pulley configuration allows for the narrowing of cables towards the humerus. It also permits the adjustment of the elbow through shoulder abduction while preserving the lines of action of each muscle.

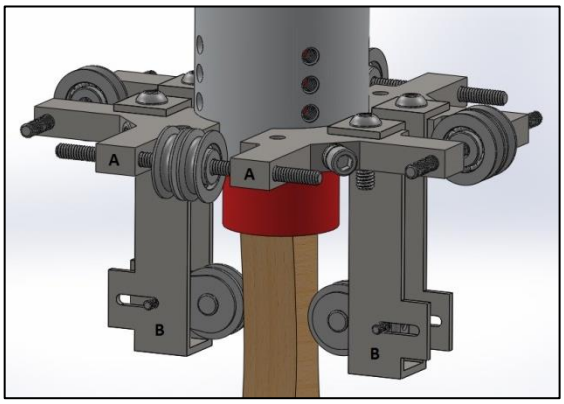

Figure 2: A) Upper Alignment System → Base Plates.
B) Lower Alignment System → Extension Brackets.

The lower alignment system is composed of two extension brackets and multiple eyebolts screwed into the bone to maintain physiological lines of action. The extension brackets are secured in between the two base plates on the anterior and posterior sides of the elbow, which corresponds to the cables connected to the Biceps and Triceps tendon respectively. Slots cut into the extension bracket allow for the shifting of the pulley closer or farther away from the humerus. This can account for any interspecimen differences in the size of the humerus that would alter the line of action of the biceps or triceps. There will be eyebolts placed into the origins of the brachialis, brachioradialis, extensor tendons, and flexor pronator mass.

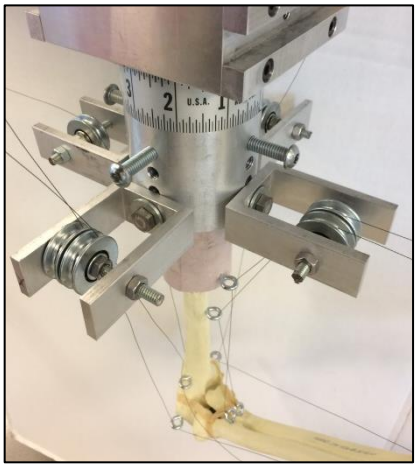

Figure 3: Prototype of Elbow Testing Apparatus

Prototype: To test the design before fabrication, a sawbones model of the elbow was potted using bondo and fixed into the cylindrical mount. Four pulley brackets represent the upper alignment and the lower alignment is represented by two eyebolts secured anteriorly and posteriorly in the potting material. Thirty-pound fishing line is used to mimic the stainless-steel cable and used to actuate the elbow. The cable will be coated in nylon to minimize friction. Additional eyebolts are inserted into the insertion sites of the biceps, brachialis, and brachioradialis to secure the fishing line to the arm. This will simulate the attachment to each tendon and transition into the cable. Once the cables are properly connected, the actuators will dynamically control the force on each cable using LabVIEW™.

Muscle Loading: According to the findings of Dunning et al. [1], the muscle loading was determined using Electromyography (EMG) [2] and physiological cross-sectional area [3] (pCSA) data. These muscle forces are directed along a path pointing from the insertion site to the origin.

Table 1: Loading Factors for Elbow in Neutral Position at 90° Flexion. (BI = Biceps, BRA = Brachialis, BRD = Brachioradialis, FPM = Flexor Pronator Mass, ET = Extensor Tendons)

Muscle	BI	BRA	BRD	TRI	FPM	ET
Muscle Contribution (% Total Load)	33.3	39.2	11.0	16.3	x	x
Load Factor	3.00	3.53	1.00	1.47	x	x
Load Value (N)	41.3	48.6	13.7	20.2	30	30

Significance: With my design and prototype, I have demonstrated the ability to flex the elbow in different angles of shoulder abduction. Using this apparatus will enable the characterization of muscle contribution to the dynamic stability of the elbow. Then once the individual muscle contributions are known, the ligamentous contribution to static stability can be determined. Furthermore, the different types of surgical procedures and their effect on stability can be investigated in vitro prior to their use in clinical applications.

References: [1] Dunning et al. J. Biomech. 2001; 34, 1039-1048. [2] Funk et al. J. Orthop. Res. 1987; 5, 529-538. [3] Amis et al. Eng. Med. 1979; 8, 41-48.

Development of a MATLAB Interface Using an Electromagnetic Tracking System for the Biomechanical Analysis of Tibiofemoral Kinematics

Joseph Greaves, Calvin Chan, Volker Musahl, Richard Debski
Department of Bioengineering, University of Pittsburgh, Pittsburgh, PA, United States. Department of Orthopaedic Surgery, University of Pittsburgh, Pittsburgh, PA, United States.

Introduction: Wide varieties of clinical exams are used to evaluate knee joint injuries. Most of these exams involve a clinician applying various forces to the knee and grading the knee positive or negative for injury. The subjective nature of the clinical exams and high variability between clinicians prove to be problematic. Thus, a need exists to evaluate clinical exams quantitatively by analyzing the 6 degrees of freedom (DOF) motion of the knee joint in order to obtain an accurate objective measurement on cadaver specimens.

Currently, an electromagnetic tracking system (Polhemus FASTRAK®, Colchester, Vermont) is used to quantify knee motion during the pivot shift exam. The current software records the anterior translation of the lateral knee compartment as well as the 6 DOF kinematics of the tibia relative to the femur. FASTRAK® has accuracies of 0.8mm and 0.15 degrees. The sampling rate is reported to be 60 Hz. However, the software used to collect the data has proven to be extremely ineffective. It requires the use of 3 separate programs to collect the necessary data. This has led to a tedious protocol and memory crashes. The objective of this project was to develop a single MATLAB GUI that can collect the tibiofemoral kinematics of the knee during the pivot shift exam using the FASTRAK®.

Design Constraints: The main constraint is that the configuration of the system settings, the data collection, and the data analysis must all be performed through MATLAB (Mathworks, 2015b Natick, MA, USA). The same accuracy that existed with the

previous system must be maintained. Memory crashes may not occur. Data should be continuously saved after each trial to prevent memory crashes.

Current Design: A single MATLAB GUI was used to create a program that has the ability to analyze the tibiofemoral kinematics of the knee. The protocol is much shorter when compared to old system.

The flowchart of the program (Figure 1) shows the required actions of the program. The first step establishes communication between the tracking system and MATLAB. Then, the system configures and activates the stylus settings. The stylus is a pen-like device used to create digital points in space. A sub- program was created to determine that the stylus was operating properly.

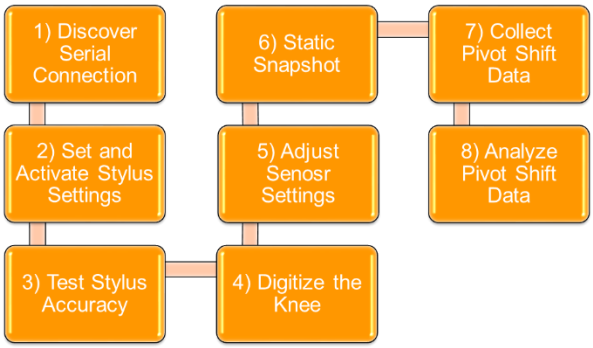

Figure 1: Map of Program

Once satisfied with the accuracy of the stylus, the user needs to digitize the knee in order to set up a coordinate system to analyze the knee kinematics. The coordinate system is created by digitizing specific bony landmarks that create anatomical axes for the tibia and the femur. Sensors are used to record the dynamic data during the performance of the clinical exams. The settings for the sensors must be configured before data can be collected.

A static snapshot must be collected in order to get the initial position of the bony landmarks (digitize points) with respect to the sensors. Finally, data is ready to be collected and analyzed.

By clicking “initialize” on the MATLAB GUI (Figure 2), a connection is established and both the settings for the stylus and the sensors are configured. The user can then begin digitizing the knee to set up a bony coordinate system, which is used to analyze kinematics. When the user is ready to collect data, they press “Start Data.” The user ends the data collection by clicking “End Data.” The data is ready to be analyzed by pressing “Analyze Data.” This generates graphs of position verses time for each of the 6 DOF as well as translation for the lateral knee compartment. The

data can then be stored safely for future use by clicking "Save Data" on the GUI.

Some steps have been taken to address the memory crashes. A matrix of zeroes has been pre- allocated to minimize the amount of RAM used during data collection. This makes data collection far more computationally efficient. In addition, data no longer has to be imported into MATLAB from external sources, which was another likely cause of memory crashes.

Discussion: The protocol has been significantly shortened by developing a single program to collect knee kinematics. Memory crashes should be eliminated because data is collected directly into MATLAB rather than being imported through another file. By subjective observation, the new program is as accurate as the previous. Both the new and the old program were used to collect the same data for each of the 6 DOF motions and the outputs were the same. Further testing may be necessary to confirm this observation.

In the future, it will be easier to collect knee kinematic data during clinical exams without having to worry about data loss. This software can be applied to joints other than the knee

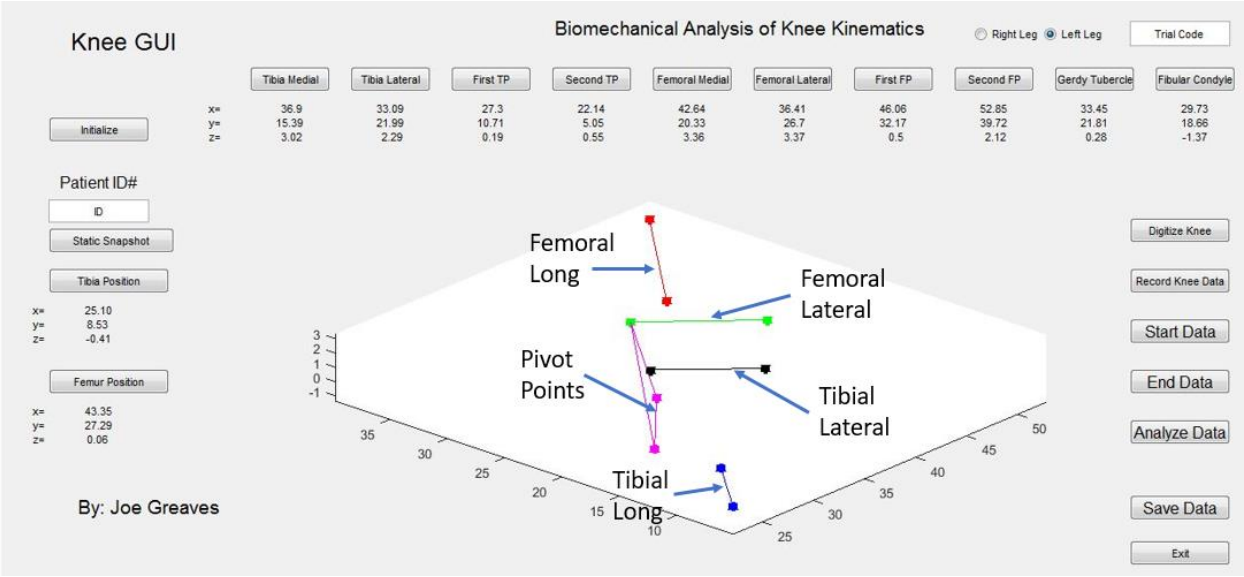

Figure 2: New MATLAB GUI